A NEW FAULT LOCATION ALGORITHM FOR USE WITH CURRENT DIFFERENTIAL PROTECTIVE RELAYS OF TWO-TERMINAL LINE

Jan Izykowski
Wroclaw University of Technology
Wroclaw, Poland
jan.izykowski@pwr.wroc.pl

Eugeniusz Rosolowski
Wroclaw University of Technology
Wroclaw, Poland
eugeniusz.rosolowski@pwr.wroc.pl

Murari Mohan Saha
ABB AB
Västerås, Sweden
murari.saha@se.abb.com

Abstract – A new fault location algorithm utilising synchronised measurements of two-end currents and one-end voltage is presented. It has been assumed that such fault location algorithm is incorporated into the current differential relay. Therefore, no additional cost for communication between the line ends is demanded and an increase of differential relay functionality is achieved. The derived fault location formula is compact and covers different fault types – what requires setting the appropriate fault type coefficients. High accuracy of fault location is assured by strict considering of the distributed parameter line model. The solution is obtained with applying iterative calculations of the Newton-Raphson method. For starting the calculations, the solutions obtained for the lumped line model are utilised. The performed ATP-EMTP evaluation prove the validity of the presented fault location algorithm and its high accuracy.

Keywords: power line, current differential relay, fault location, two-end measurement, ATP-EMTP

1 INTRODUCTION

Variety of fault location algorithms [1] has been developed so far. Different availability of the measurements is considered for them, i.e. one-end measurements [2]–[3], and much superior two-end measurements – which are acquired asynchronously [4]–[5] or synchronously [6]–[8].

This paper presents the new algorithm for locating faults on two-terminal power transmission or distribution line. It is assumed here (Fig. 1) that the fault locator (FL) is incorporated into the current differential relay from the terminal A. Besides three-phase currents ($\underline{I}_A$, $\underline{I}_B$) measured synchronously at both line ends, which are utilised by the relay, the fault locator is additionally supplied with three-phase voltage ($\underline{V}_A$) from the local line terminal. Thus, the fault locator is designed as utilising the communication infrastructure of the current differential relays, thus not demanding additional communication links. As a result, the functionality of the differential relay is greatly increased. Besides its main feature, i.e. indicating whether a fault occurred in a given protective zone or outside it, the relay provides also an information on accurate position of the fault, which is required for the inspection-repair purpose.

The fault location algorithm designed for application to current differential relay protecting a three-terminal line was introduced in [8]. However, the algorithm from [8] can not be directly applied to the two-end line. Moreover, in case of the algorithm for a three-terminal line [8], simple use of the distributed parameter line model is basically limited to analytical transfer of the signals across unfaulted line sections. In contrast, with the aim of providing high accuracy for locating faults on long lines, the distributed parameter line model in the presented algorithm is strictly utilised. Both, the voltage drop across the faulted line segment and also across the fault path resistance are determined with strict consideration of the distributed parameter line model.

The developed algorithm for locating faults on a two-terminal line is categorised to the impedance-based method, making use of the fundamental frequency voltages and currents. The algorithm is formulated using phasors of symmetrical components of the measured three-phase quantities.

For deriving the fault location algorithm, the fault loops relevant for different fault types are considered with use of the generalised fault loop model [3], in which the fault type is set with the respective complex number coefficients.

The paper starts with derivation of the fault location algorithm. Then, the results for the example fault, using the signals from ATP-EMTP [9] simulation, are presented and discussed.

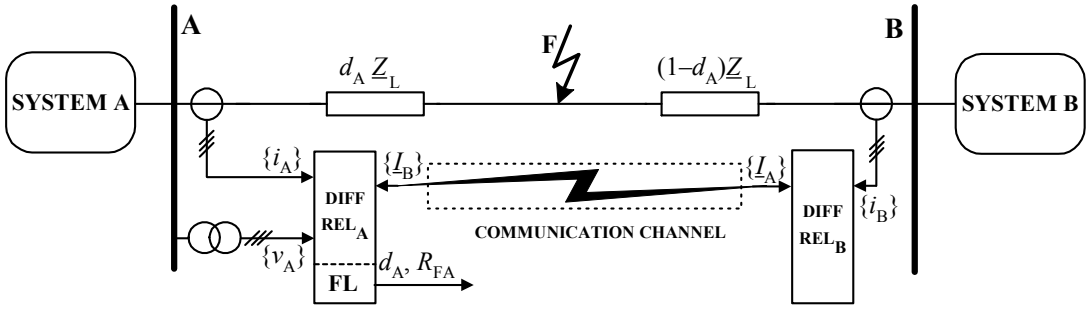

Figure 1: Fault locator (FL) associated with differential relays (DIFF REL$_A$ and DIFF REL$_B$) of two-terminal line.

2 FAULT LOCATION ALGORITHM

2.1 Generalised fault loop model

In case of availability of complete two-end measurements of voltage and current, the unknown distance to fault can be determined by processing individual symmetrical component type of the measured signals [4]–[5]. Advantages and disadvantages of applying a particular type of symmetrical components:

- positive-sequence,
- superimposed positive-sequence,
- negative-sequence or
- zero-sequence

have to be taken into account [4]–[5].

In this paper, use of incomplete two-end measurements, i.e. two-end current and one-end voltage, to fault location is considered. Due to insufficient measurement data, instead of processing the signals of the individual symmetrical component type, the natural fault loops have to be considered. Thus, accordingly to the identified fault type, the single phase loop (for phase-to-ground faults) and inter-phase loop (for faults involving two or three phases) have to be considered. The fault loop contains the section of the line from the measuring point up to the fault point and the fault path resistance.

The generalised fault loop model [3] is applied for determining the distance to fault. In further considerations the case of the fault locator FL (Fig.1) incorporated to the differential relay at the bus A is taken into account. The algorithm for the other case, with the fault locator at the side B relay, can be formulated analogously. In the considered case, the generalised model describes the fault loop seen from the line end A:

$$\underline{V}_{\mathrm{AFp}}(d_{\mathrm{A}}) - R_{\mathrm{FA}}\underline{I}_{\mathrm{F}} = 0 \qquad (1)$$

where:

$\underline{V}_{\mathrm{AFp}}(d_{\mathrm{A}})$ – fault loop voltage composed accordingly to the fault type, obtained after the analytic transfer from the bus A to the fault point F,

d_{A} – unknown distance from bus A to fault (p.u.),

R_{FA} – fault path resistance,

$\underline{I}_{\mathrm{F}}$ – total fault current (fault path current).

2.2 Fault loop voltage at fault point

The transfer of the fault loop voltage from the bus A to the fault point F is equivalent to subtracting the voltage drop across the faulted line section (part of the loop between the bus A and the fault point F) from the original fault loop voltage at the bus A. The transferred fault loop voltage can be composed as the following weighted sum of the respective symmetrical components:

$$\underline{V}_{\mathrm{AFp}}(d_{\mathrm{A}}) = \underline{\mathrm{a}}_1\underline{V}_{\mathrm{F1}}(d_{\mathrm{A}}) + \underline{\mathrm{a}}_2\underline{V}_{\mathrm{F2}}(d_{\mathrm{A}}) + \underline{\mathrm{a}}_0\underline{V}_{\mathrm{F0}}(d_{\mathrm{A}}) \qquad (2)$$

where:

subscripts denoting the component type are as follows: 1 – positive-, 2 – negative-, 0 – zero-sequence,

$\underline{\mathrm{a}}_1$, $\underline{\mathrm{a}}_2$, $\underline{\mathrm{a}}_0$ – weighting coefficients dependent on fault type [3], as gathered in Table 1.

FAULT	$\underline{\mathrm{a}}_1$	$\underline{\mathrm{a}}_2$	$\underline{\mathrm{a}}_0$
a-g	1	1	1
b-g	$\underline{\mathrm{a}}^2$	$\underline{\mathrm{a}}$	1
c-g	$\underline{\mathrm{a}}$	$\underline{\mathrm{a}}^2$	1
a-b, a-b-g a-b-c, a-b-c-g	$1-\underline{\mathrm{a}}^2$	$1-\underline{\mathrm{a}}$	0
b-c, b-c-g	$\underline{\mathrm{a}}^2-\underline{\mathrm{a}}$	$\underline{\mathrm{a}}-\underline{\mathrm{a}}^2$	0
c-a, c-a-g	$\underline{\mathrm{a}}-1$	$\underline{\mathrm{a}}^2-1$	0
$\underline{\mathrm{a}} = \exp(\mathrm{j}2\pi/3)$; $\mathrm{j} = \sqrt{-1}$			

Table 1: Weighting coefficients for composing signal (2).

Applying the distributed parameter line model [5], the symmetrical components of voltages from (2) are determined as follows:

$$\underline{V}_{\mathrm{F1}}(d_{\mathrm{A}}) = \underline{V}_{\mathrm{A1}}\cosh(\underline{\gamma}_1\ell d_{\mathrm{A}}) - \underline{Z}_{\mathrm{c1}}\underline{I}_{\mathrm{A1}}\sinh(\underline{\gamma}_1\ell d_{\mathrm{A}}) \qquad (3)$$

$$\underline{V}_{\mathrm{F2}}(d_{\mathrm{A}}) = \underline{V}_{\mathrm{A2}}\cosh(\underline{\gamma}_1\ell d_{\mathrm{A}}) - \underline{Z}_{\mathrm{c1}}\underline{I}_{\mathrm{A2}}\sinh(\underline{\gamma}_1\ell d_{\mathrm{A}}) \qquad (4)$$

$$\underline{V}_{\mathrm{F0}}(d_{\mathrm{A}}) = \underline{V}_{\mathrm{A0}}\cosh(\underline{\gamma}_0\ell d_{\mathrm{A}}) - \underline{Z}_{\mathrm{c0}}\underline{I}_{\mathrm{A0}}\sinh(\underline{\gamma}_0\ell d_{\mathrm{A}}) \qquad (5)$$

where:

$\underline{V}_{\mathrm{A1}}$, $\underline{V}_{\mathrm{A2}}$, $\underline{V}_{\mathrm{A0}}$ – symmetrical components of side A voltages,

$\underline{I}_{\mathrm{A1}}$, $\underline{I}_{\mathrm{A2}}$, $\underline{I}_{\mathrm{A0}}$ – symmetrical components of side A currents,

ℓ – length of the line (km),

$\underline{\gamma}_1 = \sqrt{\underline{Z}'_{1\mathrm{L}}\underline{Y}'_{1\mathrm{L}}}$ – propagation constant of the line for the positive- (negative-) sequence,

$\underline{\gamma}_0 = \sqrt{\underline{Z}'_{0\mathrm{L}}\underline{Y}'_{0\mathrm{L}}}$ – propagation constant of the line for the zero-sequence,

$\underline{Z}_{\mathrm{c1}} = \sqrt{\underline{Z}'_{1\mathrm{L}}/\underline{Y}'_{1\mathrm{L}}}$ – characteristic impedance of the line for the positive-sequence (negative-sequence),

$\underline{Z}_{\mathrm{c0}} = \sqrt{\underline{Z}'_{0\mathrm{L}}/\underline{Y}'_{0\mathrm{L}}}$ – characteristic impedance of the line for the zero-sequence,

$\underline{Z}'_{1\mathrm{L}} = R'_{1\mathrm{L}} + \mathrm{j}\omega_1 L'_{1\mathrm{L}}$ – impedance of the line for the positive-sequence (negative-sequence) (Ω/km),

$\underline{Z}'_{0\mathrm{L}} = R'_{0\mathrm{L}} + \mathrm{j}\omega_1 L'_{0\mathrm{L}}$ – impedance of the line for the zero-sequence (Ω/km),

$\underline{Y}'_{1\mathrm{L}} = G'_{1\mathrm{L}} + \mathrm{j}\omega_1 C'_{1\mathrm{L}}$ – admittance of the line for the positive-sequence (negative-sequence) (S/km),

$\underline{Y}'_{0\mathrm{L}} = G'_{0\mathrm{L}} + \mathrm{j}\omega_1 C'_{0\mathrm{L}}$ – admittance of the line for the zero-sequence (S/km),

$R'_{1\mathrm{L}}$, $L'_{1\mathrm{L}}$, $G'_{1\mathrm{L}}$, $C'_{1\mathrm{L}}$ – resistance, inductance, conductance and capacitance of the line for the positive-sequence (negative-sequence) per km length,

$R'_{0\mathrm{L}}$, $L'_{0\mathrm{L}}$, $G'_{0\mathrm{L}}$, $C'_{0\mathrm{L}}$ – resistance, inductance, conductance and capacitance of the line for the zero-sequence per km length.

The line parameters for the positive- and negative-sequences are identical and therefore they are uniformly denoted with '1' in the subscripts for both sequences.

2.3 Total fault current

Summing of phase currents (a, b, c in the subscripts) from both line ends (A, B in the subscripts) appears as the simplest way of determining the fault current in particular phases at the fault point:

$$\underline{I}_{\mathrm{Fa}} = \underline{I}_{\mathrm{Aa}} + \underline{I}_{\mathrm{Ba}} \tag{6}$$

$$\underline{I}_{\mathrm{Fb}} = \underline{I}_{\mathrm{Ab}} + \underline{I}_{\mathrm{Bb}} \tag{7}$$

$$\underline{I}_{\mathrm{Fc}} = \underline{I}_{\mathrm{Ac}} + \underline{I}_{\mathrm{Bc}} \tag{8}$$

Then, one can use these currents (6)–(8) for composing the total fault current, accordingly to the fault type. However, this way of the composing reveals as affected by the currents charging line shunt capacitances. This is so, since in (6)–(8) the currents from the line ends are summed, and not the currents flowing from both sides directly into to the fault point. The currents summed in (6)–(8) on the way from the line ends (A, B) to the fault point (F) are lessen by the currents charging line shunt capacitances. This is the explanation why the natural way of determining the fault currents as in (6)–(8) will not be longer used. Instead, the detailed analysis of the flow of currents in the faulted line will be considered.

Taking into account the share of individual symmetrical components (1 – positive-, 2 – negative-, 0 – zero-sequence, respectively) of the total fault current ($\underline{I}_{\mathrm{F1}}$, $\underline{I}_{\mathrm{F2}}$, $\underline{I}_{\mathrm{F0}}$) in the total fault current ($\underline{I}_{\mathrm{F}}$) one obtains [3]:

$$\underline{I}_{\mathrm{F}} = \underline{a}_{\mathrm{F1}}\underline{I}_{\mathrm{F1}} + \underline{a}_{\mathrm{F2}}\underline{I}_{\mathrm{F2}} + \underline{a}_{\mathrm{F0}}\underline{I}_{\mathrm{F0}} \tag{9}$$

where:

$\underline{a}_{\mathrm{F1}}$, $\underline{a}_{\mathrm{F2}}$, $\underline{a}_{\mathrm{F0}}$ – share coefficients, dependent on fault type and the assumed preference with respect to using particular sequences (the recommended set is delivered in Table 2).

FAULT	$\underline{a}_{\mathrm{F1}}$	$\underline{a}_{\mathrm{F2}}$	$\underline{a}_{\mathrm{F0}}$
a–g	0	3	0
b–g	0	$3\underline{a}$	0
c–g	0	$3\underline{a}^2$	0
a–b	0	$1-\underline{a}$	0
b–c	0	$\underline{a}-\underline{a}^2$	0
c-a	0	$\underline{a}^2-1$	0
a-b-g	$1-\underline{a}^2$	$1-\underline{a}$	0
b-c-g	$\underline{a}^2-\underline{a}$	$\underline{a}-\underline{a}^2$	0
c-a-g	$\underline{a}-1$	$\underline{a}^2-1$	0
a-b-c, a-b-c-g	$1-\underline{a}^2$	$1-\underline{a}$ *)	0
*) – there is no negative sequence component under these faults and the coefficient can be assumed as equal to zero			

Table 2: Share coefficients for composing total fault current.

There is a possibility of applying different, alternative sets of the share coefficients [3], however, the coefficients for which the zero-sequence is eliminated ($\underline{a}_{\mathrm{F0}} = 0$) – as in Table 2, is recommended for the considered fault location algorithm. In this way, use of the line parameters for the zero-sequence – which are considered as unreliable data, is avoided for determining the total fault current. This is advantageous for assuring the highest possible accuracy of fault location.

One can notice that, when using the share coefficients proposed in Table 2, the preference of using the negative-sequence over the positive-sequence is set for single-phase and phase-to-phase faults.

Accurate determination of the symmetrical components of the total fault current can be performed with strict consideration of the distributed parameter model of the faulted line. Such models for the positive-sequence and negative-sequence are presented in Fig. 2. Taking these models into the consideration, one derives (the derivation is provided in Appendix) the following formula for the *i*-th symmetrical component of the total fault current:

$$\underline{I}_{\mathrm{F}i} = \frac{\underline{M}_i}{\cosh(\underline{\gamma}_1 \ell(1-d_{\mathrm{A}}))} \tag{10}$$

where:

$$\underline{M}_i = \underline{I}_{\mathrm{B}i} + \underline{I}_{\mathrm{A}i}\cosh(\underline{\gamma}_1\ell) - \frac{\underline{V}_{\mathrm{A}i}}{\underline{Z}_{\mathrm{c1}}}\sinh(\underline{\gamma}_1\ell) \tag{11}$$

i=1: positive-sequence or *i*=2: negative-sequence.

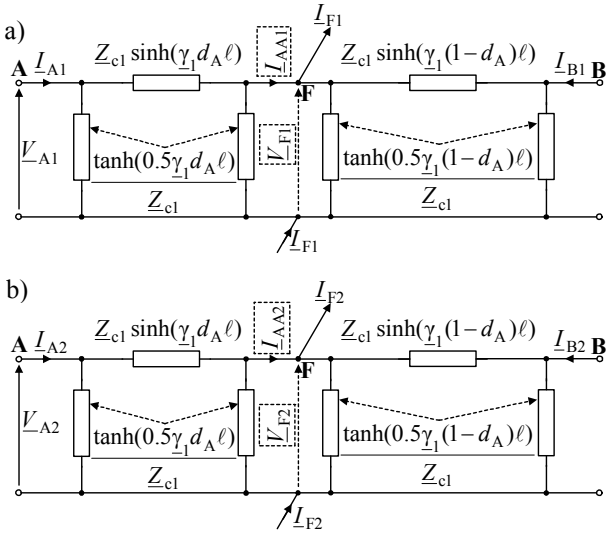

Figure 2: Equivalent circuit diagram of faulted line for: a) positive-sequence, b) negative-sequence; (the signals used in the derivation (delivered in Appendix) are marked by the dashed boxes).

The obtained formula (10) for the *i*-th symmetrical component of the total fault current is compact and the unknown distance to fault (d_{A}) is involved in the denominator of (10) only.

Substituting the positive- and negative-sequence components of the total fault current, determined in [10]–[11], into (9), and also taking into account that the

zero-sequence is eliminated (Table2), one obtains the total fault current in the form:

$$\underline{I}_{\mathrm{F}} = \frac{\underline{\mathrm{a}}_{\mathrm{F1}}\underline{M}_1 + \underline{\mathrm{a}}_{\mathrm{F2}}\underline{M}_2}{\cosh(\underline{\gamma}_1 \ell(1-d_{\mathrm{A}}))} \tag{12}$$

where:

$\underline{M}_1$, $\underline{M}_2$ – quantities defined in (11),

$\underline{\mathrm{a}}_{\mathrm{F1}}$, $\underline{\mathrm{a}}_{\mathrm{F2}}$ – share coefficients gathered in Table 2.

2.4 Fault location formula

Substitution of the total fault current (12) into the generalised fault loop model (1) gives:

$$\underline{V}_{\mathrm{AFp}}(d_{\mathrm{A}}) - R_{\mathrm{FA}} \frac{\underline{\mathrm{a}}_{\mathrm{F1}}\underline{M}_1 + \underline{\mathrm{a}}_{\mathrm{F2}}\underline{M}_2}{\cosh(\underline{\gamma}_1 \ell(1-d_{\mathrm{A}}))} = 0 \tag{13}$$

and finally:

$$\underline{V}_{\mathrm{AFp}}(d_{\mathrm{A}}) \cdot \cosh(\underline{\gamma}_1 \ell(1-d_{\mathrm{A}})) - R_{\mathrm{FA}}(\underline{\mathrm{a}}_{\mathrm{F1}}\underline{M}_1 + \underline{\mathrm{a}}_{\mathrm{F2}}\underline{M}_2) = 0 \tag{14}$$

where:

$\underline{V}_{\mathrm{AFp}}(d_{\mathrm{A}})$ – defined in (2)–(5), with use of the weighting coefficients specified for different faults in Table 1,

$\underline{M}_1$, $\underline{M}_2$ – quantities defined in (11),

$\underline{\mathrm{a}}_{\mathrm{F1}}$, $\underline{\mathrm{a}}_{\mathrm{F2}}$ – share coefficients dependent on the fault type, as gathered in Table 2.

The derived fault location formula (14) is compact and covers different fault types, what requires setting the appropriate fault type coefficients, as provided in Table 1 and in Table 2.

There are two unknowns in the fault location formula (14): distance to fault d_{A} and fault resistance R_{FA}. After resolving (14) into the real and imaginary parts, one of the known numeric procedures for solving nonlinear equations can be applied. It has been checked that the Newton-Raphson iterative method [5] is a good choice for that.

Applying the Newton-Raphson method, the start of iterative calculations can be performed with the initial values for the unknowns: d_{A}^0, R_{FA}^0, denoted with the superscript 0 (iteration number: 0, as the starting point for the 1st iteration of the calculations). These values can be calculated from the fault location formula (14) adapted to the lumped line model with neglecting shunt capacitances. This can be accomplished by introducing to (14) the substitutions: $\cosh(x) \rightarrow 1$, $\sinh(x) \rightarrow 0$, where x is an argument of the considered hyperbolic trigonometric function. As a result, one obtains the following simplified fault location formula:

$$\underline{V}_{\mathrm{Ap}} - d_{\mathrm{A}}^0 \underline{Z}_{1\mathrm{L}} \underline{I}_{\mathrm{Ap}} - R_{\mathrm{FA}}^0 \underline{M}_{12}^0 = 0 \tag{15}$$

with the fault loop voltage and current from the line end A, defined for the lumped line model with neglected shunt capacitances:

$$\underline{V}_{\mathrm{Ap}} = \underline{\mathrm{a}}_1 \underline{V}_{\mathrm{A1}} + \underline{\mathrm{a}}_2 \underline{V}_{\mathrm{A2}} + \underline{\mathrm{a}}_0 \underline{V}_{\mathrm{A0}} \tag{16}$$

$$\underline{I}_{\mathrm{Ap}} = \underline{\mathrm{a}}_1 \underline{I}_{\mathrm{A1}} + \underline{\mathrm{a}}_2 \underline{I}_{\mathrm{A2}} + \underline{\mathrm{a}}_0 \frac{\underline{Z}_{0\mathrm{L}}}{\underline{Z}_{1\mathrm{L}}} \underline{I}_{\mathrm{A0}} \tag{17}$$

where:

$$\underline{M}_{12}^0 = \underline{\mathrm{a}}_{\mathrm{F1}} \underline{I}_{\mathrm{A1}} + \underline{\mathrm{a}}_{\mathrm{F2}} \underline{I}_{\mathrm{A2}}$$

$$\underline{Z}_{1\mathrm{L}} = \underline{Z}'_{1\mathrm{L}} \ell\,, \quad \underline{Z}_{0\mathrm{L}} = \underline{Z}'_{0\mathrm{L}} \ell\,.$$

Resolving (15) into the real and imaginary parts, the following compact formula for the distance to fault, after eliminating the unknown fault resistance, is obtained:

$$d_{\mathrm{A}}^0 = \frac{\mathrm{real}(\underline{V}_{\mathrm{Ap}}) \cdot \mathrm{imag}(\underline{M}_{12}^0) - \mathrm{imag}(\underline{V}_{\mathrm{Ap}}) \cdot \mathrm{real}(\underline{M}_{12}^0)}{\mathrm{real}(\underline{Z}_{1\mathrm{L}} \underline{I}_{\mathrm{Ap}}) \cdot \mathrm{imag}(\underline{M}_{12}^0) - \mathrm{imag}(\underline{Z}_{1\mathrm{L}} \underline{I}_{\mathrm{Ap}}) \cdot \mathrm{real}(\underline{M}_{12}^0)} \tag{18}$$

Having calculated the distance to fault (18), one can calculate the other unknown, i.e. the fault resistance. As for example, from the real part of (15) one gets:

$$R_{\mathrm{FA}}^0 = \frac{\mathrm{real}(\underline{V}_{\mathrm{Ap}}) - d_{\mathrm{A}}^0 \mathrm{real}(\underline{Z}_{1\mathrm{L}} \underline{I}_{\mathrm{Ap}})}{\mathrm{real}(\underline{M}_{12}^0)} \tag{19}$$

In practice, for the line lengths up to 150 km, the simple formulae (18)–(19) can be utilised. However, in order to assure high accuracy of fault location on longer lines, the Newton-Raphson solution of (14), resolved earlier into the real and imaginary parts, has to be applied. The results obtained from (18)–(19) are used for starting these iterative calculations.

3 ATP-EMTP ALGORITHM EVALUATION

The derived fault location algorithm has been tested and evaluated with the fault data obtained from versatile ATP-EMTP [9] simulations of faults in the power network containing the 400 kV, 300 km transmission line.

The line impedances were assumed as:

$\underline{Z}_{1\mathrm{L}}$=(8.28+j94.5) Ω, $\underline{Z}_{0\mathrm{L}}$=(82.5+j307.9) Ω,

and the line capacitances:

$C_{1\mathrm{L}}$=13 nF/km, $C_{0\mathrm{L}}$=8.5 nF/km.

The equivalent supplying systems were modelled with impedances:

$\underline{Z}_{1\mathrm{SA}}$ =(1.312+j15.0) Ω , $\underline{Z}_{0\mathrm{SA}}$ =(2.334+j26.6) Ω,

$\underline{Z}_{1\mathrm{SB}}$=2$\underline{Z}_{1\mathrm{SA}}$, $\underline{Z}_{0\mathrm{SB}}$=2$\underline{Z}_{0\mathrm{SA}}$,

the e.m.f. of the system B was delayed by 30° with respect to the system A.

At the first step of the evaluation, current and voltage instrument transformers, ideally transforming the signals from a power system, were reflected in the simulation model. Use of the idealised instrument transformers was intentionally assumed with the aim of investigation of the errors of the developed fault location algorithm alone. Then, the instrument transformers with typical parameters were included into the simulation model.

The analogue low-pass filters with 350 Hz cut-off frequency were also included. The sampling frequency of 1000 Hz was applied and the phasors were determined with use of the DFT algorithm. The obtained continuous time results for the distance to fault and fault resistance were averaged within the post-fault interval: from 30 up to 50 ms.

Fig. 3 presents the waveforms of the fault locator input signals (Fig. 3a–Fig. 3c) and the fault location results (Fig. 3d–Fig. 3f) for the example fault.

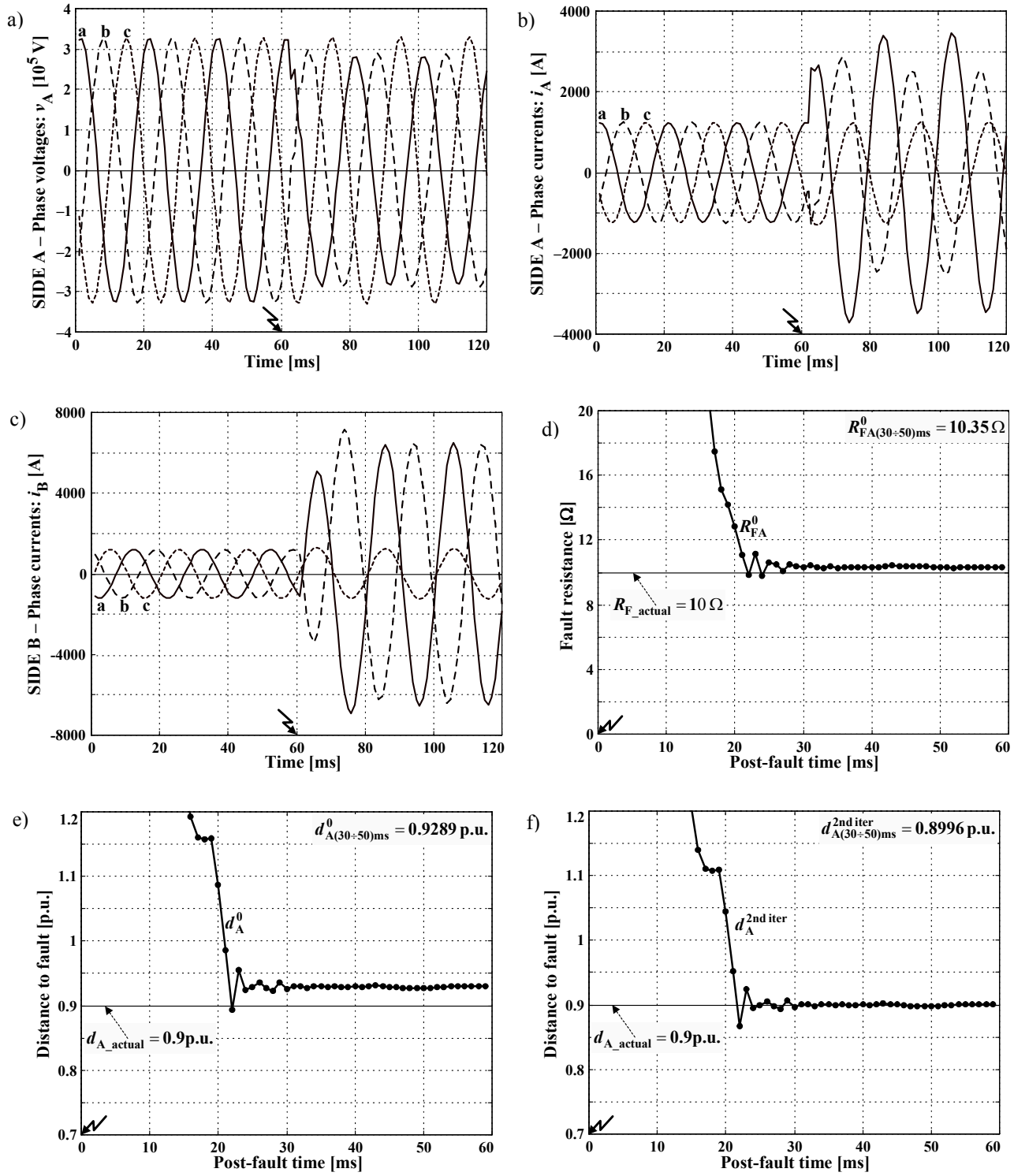

Figure 3: The fault location example: a) three-phase voltage from the end A, b) three-phase current from the end A, c) three-phase current from the end B, d) fault resistance (lumped line model), e) distance to fault (lumped line model), e) distance to fault (2nd iteration for distributed parameter line model).

The considered example fault has the following specifications:

- fault type: a-b-g,
- fault location: d_{A_actual}=0.9 p.u.,
- fault resistance: R_{F_actual}=10 Ω.

Applying the formulae (18)–(19) of the lumped line model, the estimated fault resistance takes (after the averaging) the value: $R^0_{FA(30\div50)ms} = 10.35\,\Omega$ (Fig. 3d) and the distance to fault: $d^0_{A(30\div50)ms} = 0.9289$ p.u. The error in estimating the fault resistance is not important since information on resistance involved in the fault is only informative. In case of estimating the distance to fault, the error takes the value equal to around 3%. In

order to improve fault location accuracy, the formula (14) is solved iteratively, and after performing two iterations (superscript: '2nd iter') of the calculations, very accurate result: $d_{\mathrm{A}(30\div50)\mathrm{ms}}^{\text{2nd iter}} = 0.8996$ p.u. is obtained.

Different specifications of faults and pre-fault power flows have been considered in the evaluation of the accuracy of the developed fault location accuracy. For the faults involving fault resistance up to 10 Ω, the maximum errors do not exceed: 0.15% for the case of the instrument transformers with ideal transformation and 1% with the real instrument transformers included.

4 CONLUSIONS

The new fault location algorithm, utilising synchronised measurements of two-end currents and one-end voltage, has been derived. Such availability of measurements is of practical importance since the developed algorithm is considered as to be incorporated into the current differential relay.

The presented fault location algorithm has been derived for the transposed line using the symmetrical components approach. There is also a possibility for reformulating the algorithm to the untransposed line case.

The derived fault location formula is compact and covers different fault types, what requires setting the appropriate fault type coefficients. The distributed parameter line model is strictly taken into account, what assures very high accuracy of fault location. For lines of the length shorter than 150 km, very simple formulae can be utilised.

The ATP-EMTP simulation results show that the accuracy of location with the presented algorithm is very high under various fault types, fault resistances, fault locations, pre-fault flows and source impedances. The maximum error is below 1%.

5 APPENDIX – DERIVATION OF (10)–(11)

The formulae (10)–(11) apply for both the positive- and negative-sequence. Derivation of them for both sequences is analogous and let us derive them for one of the sequences, for example for the positive-sequence.

According to the distributed parameter model of the line for the positive-sequence (Fig. 2a) one obtains after considering the faulted line section A-F:

$$\underline{V}_{\mathrm{F1}} = \underline{V}_{\mathrm{A1}}\cosh(\underline{\gamma}_1 \ell d_{\mathrm{A}}) - \underline{Z}_{\mathrm{c1}}\underline{I}_{\mathrm{A1}}\sinh(\underline{\gamma}_1 \ell d_{\mathrm{A}}) \qquad \text{(A1)}$$

$$\underline{I}_{\mathrm{AA1}} = -\frac{\underline{V}_{\mathrm{A1}}}{\underline{Z}_{\mathrm{c1}}}\sinh(\underline{\gamma}_1 \ell d_{\mathrm{A}}) + \underline{I}_{\mathrm{A1}}\cosh(\underline{\gamma}_1 \ell d_{\mathrm{A}}) \qquad \text{(A2)}$$

Considering the remaining line section F-B with taking the transferred signals (A1)–(A2), one obtains the following formula for the positive-sequence of the remote current $\underline{I}_{\mathrm{B1}}$ (note that the direction of this current is opposite with respect to the current $\underline{I}_{\mathrm{A1}}$):

$$\underline{I}_{\mathrm{B1}} = \frac{\underline{V}_{\mathrm{F1}}}{\underline{Z}_{\mathrm{c1}}}\sinh(\underline{\gamma}_1 \ell(1-d_A)) - (\underline{I}_{\mathrm{AA1}} - \underline{I}_{\mathrm{F1}})\cosh(\underline{\gamma}_1 \ell(1-d_A)) \qquad \text{(A3)}$$

Substituting voltage $\underline{V}_{\mathrm{F1}}$ (determined in (A1)) and current $\underline{I}_{\mathrm{AA1}}$ (determined in (A2)) into (A3), after tedious rearrangements – performed with applying the following identities for hyperbolic functions:

$$\sinh(x+y) = \sinh(x)\cosh(y) + \cosh(x)\sinh(y) \qquad \text{(A4)}$$

$$\cosh(x+y) = \sinh(x)\sinh(y) + \cosh(x)\cosh(y) \qquad \text{(A5)}$$

one obtains the following formula for the positive-sequence component of the total fault current:

$$\underline{I}_{\mathrm{F1}} = \frac{\underline{M}_1}{\cosh(\underline{\gamma}_1 \ell(1-d_{\mathrm{A}}))} \qquad \text{(A6)}$$

where:

$$\underline{M}_1 = \underline{I}_{\mathrm{Bl}} + \underline{I}_{\mathrm{A1}}\cosh(\underline{\gamma}_1 \ell) - \frac{\underline{V}_{\mathrm{A1}}}{\underline{Z}_{\mathrm{c1}}}\sinh(\underline{\gamma}_1 \ell) \qquad \text{(A7)}$$

The obtained formulae (A6)–(A7) are consistent with (10)–(11).

REFERENCES

[1] IEEE Std C37.114: "IEEE Guide for Determining Fault Location on AC Transmission and Distribution Lines", IEEE Power Engineering Society Publ., pp. 1-42, 8 June 2005

[2] L. Eriksson, M.M. Saha and G.D. Rockefeller, "An accurate fault locator with compensation for apparent reactance in the fault resistance resulting from remote-end infeed", IEEE Trans. on PAS, vol. PAS-104, pp. 424-436, No. 2, 1985

[3] J. Izykowski, E. Rosolowski and M.M. Saha, "Locating faults in parallel transmission lines under availability of complete measurements at one end", *IEE Generation, Transmission and Distribution*, Vol. 151, No. 2, pp. 268–273, 2004.

[4] D. Novosel, D.G. Hart, E. Udren and J. Garitty, "Unsynchronized two-terminal fault location estimation", IEEE Trans. on Power Delivery, vol. 11, pp. 130–138, No. 1, 1996

[5] J. Izykowski, R. Molag, E. Rosolowski and M.M. Saha, "Accurate location of faults on power transmission lines with use of two-end unsynchronized measurements" IEEE Trans. on Power Delivery, Vol. 21, No. 2, pp. 627–633, April 2006

[6] IEEE Std. C37.118: "IEEE Standard for Synchrophasors for Power Systems", IEEE Power Engineering Society Publ., pp. 1-65, 22 March 2006

[7] M. Kezunovic and B. Perunicic, "Automated transmission line fault analysis using synchronized sampling at two ends", IEEE Trans. on Power Systems, pp 441–447, PS–11, 1996

[8] J. Izykowski, E. Rosolowski, M.M. Saha, M. Fulczyk and P. Balcerek, "A fault location method for application with current differential relays of three-terminal lines", IEEE Trans. on Power Delivery, Vol. 22, No. 4, pp. 2099–2107, October 2007

[9] H. Dommel, "Electro-Magnetic Transients Program", BPA, Portland, Oregon, 1986.